View metadata, citation and similar papers at core.ac.uk

brought to you by CORE

provided by Sabanci University Research Database

Micro Position Control of a Designed 3-PRR Compliant Mechanism Using Experimental Models

Merve Acer
Mechanical Engineering
Istanbul Technical University
Istanbul, Turkey
acerm@itu.edu.tr

Asif Sabanovic
Mechatronics Engineering
Sabanci University
Istanbul, Turkey
asif@sabanciuniv.edu

***Abstract*— A new compliant stage based on 3-PRR kinematic structure is designed to be used as a planar micro positioner. The mechanism is actuated by using piezoelectric actuators and center position of the stage is measured using a dual laser position sensor. It's seen that manufactured mechanism has unpredictable motion errors due to manufacturing and assembly faults. Thus, sliding mode control with disturbance observer is chosen to be implemented as position control in x-y axes of the center of the mechanism. Instead of piezoelectric actuator models, experimental models are extracted for each actuation direction in order to be used as nominal plants for the disturbance observer. The position control results are compared with the previous position control using linear piezoelectric actuator models and it's seen that the implemented control methodology is better in terms of errors in x and y axes. Besides, the position errors are lowered down to ±0.06 microns, which is the accuracy of the dual laser position sensor.**

Keywords*— *compliant mechanism, micro motion mechanisms, sliding mode control, piezoelectric actuator, observer

I. INTRODUCTION

In modern technology, positioning mechanical components become very important for micro/nano applications such as cell manipulation, surgery, aerospace, micro fluidics, optical systems, micro machining and micro assembly etc. [1-2]. As a result of these technologies high precision positioning devices with controlled motions at sub-micron level is needed. The need of increased accuracy and precision requires the development of design and control methods simple enough that can be used in engineering practice. Traditional rigid body mechanisms started not to provide needed micron range, accuracy and precision. Then, high precision mechanisms with flexible joints are designed in which flexible joints transfer necessary motion or force in the mechanism. The desired motion is provided with the deflection of these flexible joints called in the literature as "flexures" and the mechanisms which are composed of flexures instead of rigid joints are called "compliant mechanisms" [3]. These mechanisms have many advantages to be used in high precision applications. The most important advantages can be listed as: providing high resolution, frictionless, smooth and continuous motion, enabling small displacements up to 0.01 µm with submicron accuracy, being insensitive to temperature changes if they have a symmetrical structure, providing weight reduction, being compact and lastly, being cheaper than the high precision mechanisms that use conventional rigid joints because of the manufacturing costs.

A compliant planar parallel mechanism is decided to be designed in the light of these advantages. The motivation for this work is to design micro positioning of necessary parts in x-y axes for the micro system applications in Sabancı University Laboratory. As an example, one of these applications is the laser micro machining unit as shown in Fig. 1 [4]. The stage is thought to be used as a fine positioner on the top of a coarse positioner so that smaller pieces can be cut or manipulated more precisely.

Mostly parallel kinematic structures are used for micro positioning stages because of their advantages but parallel kinematic structures have also important disadvantages such as having limited workspace and dexterity, non-linear kinematics, difficult calculation of forward kinematics. However these drawbacks are not problematic for flexure based (compliant) mechanisms because the motions are in micro range. In addition, due to the small flexure displacements the kinematics can be assumed as linear in the workspace range. The repeatability of these structures is eliminated with flexures because there is no backlash and friction problem in the joints as in rigid mechanisms.

Various types of parallel kinematic structures have been used while designing compliant positioning stages in the literature. These structures are based on popular rigid body parallel mechanisms. A lot of planar parallel compliant mechanisms have been designed based on triangular stages. The most common kinematic structure that is used in compliant mechanisms is 3-RRR [5-11]. The triangular stage is actuated by three linkages connected to each other with three revolute joints. The end-effector has translation motion along x-y direction and a rotation about the z axis. This type of parallel kinematic structure amplifies the motion of the actuators. The revolute joints were replaced with flexure hinges which were designed according to the desired parallel kinematic performance. Another triangular stage has 3-PRR kinematic structure which is composed of 1 prismatic, 2 revolute joints is used in [12] as a compliant mechanism.

978-1-4673-5769-2/13/$31.00 ©2013 IEEE

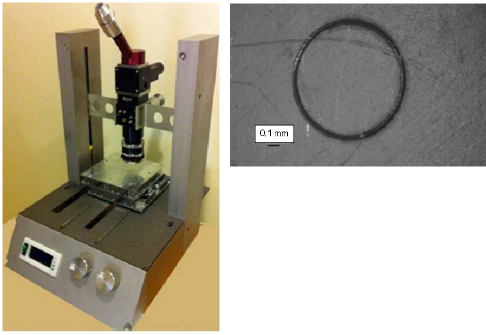

Fig. 1. Laser micro machining unit [4].

The position tracking control of the compliant micro motion stages is very important because of the high performance requirements in high precision applications. The complexity of modeling of these mechanisms leads to be hard to control its position due to a lack of accurate model since it is difficult to compute. Therefore, a usable method should be defined for controlling the mechanism or the control should eliminate the nonlinearities and uncertainties of the mechanism that is coming from manufacturing and assembly errors. There are researches going on simplifying the models that can be computed while real time control is running. The most popular one is pseudo rigid body model which computes the stiffness value of the flexures that are equivalent to joints with torsional springs and rest of the mechanism is treated as a rigid body mechanism [13]. Howell and Mathilda have developed loop closure theory which uses the complex number method to model the mechanism [14]. Handley et al. have used this model to make the position control of the mechanism [15]. A linear scheme method is presented by Her and Chang for the displacement analysis of micro positioning stages which linearize the geometric constraint equations of the stages [16]. Zhang et al. developed the work and came up with the idea of constant Jacobian method for computing the kinematics of the mechanism [17]. This method had been used for the PID control of a 3-RRR flexure based mechanism [18]. Goldfrab has only made the position control simulation of a compliant mechanism by using a sliding mode control [19]. A four bar mechanism is designed for micro/nano manipulation and a robust adaptive control methodology is applied by Liaw et al [20]. Another adaptive control has been used by Shieh and Huang to emulate the unwanted behaviors of the mechanism [21]. Chang et al. have designed a x-y-θz piezo micro positioner and used a feedback control to eliminate the hysteresis, nonlinearity and drift of piezoelectric effects [22].

A different control method which is Sliding Mode Control (SMC) with Disturbance Observer (DOB) based on SMC to remove the unpredictable errors caused by manufacturing and assembly errors are presented for the newly designed 3-PRR compliant mechanism in our laboratory in [23]. The reason why SMC is selected as the control method is that it has disturbance rejection and insensitivity to parameter variations. In this work, the position control of the mechanism is improved by using experimentally extracted models for each actuation direction instead of using piezoelectric actuator linear nominal models used for DOB in [23]. The accuracy of the mechanism has reached to the measurement that is used.

In section II the 3-PRR compliant stage is introduced, the methodology of the control method is presented in sec. III, the experimental setup and the transformation matrix which connects the end-effector x-y motion with the displacement vectors coming from piezoelectric actuators is explained in sec. IV. Finally the results are presented in sec. V and a conclusion has been made based on the results in sec. VI.

II. 3-PRR Compliant Mechanism

The compliant stage is designed to be used as a high precision planar positioning stage for the laser micro machining application in our laboratory. The main design criterias for the mechanism are to be stiff enough for the unwanted axes motions and give us opportunity to be controlled easily. According to those limitations we have selected a 3-PRR (one prismatic – two revolute joints for each link) kinematic structure shown in Fig. 2a which has a compact shape, decouples the stiffness between actuators, improves the stiffness which leads to the parasitic motions. The main difference of our 3-PRR compliant mechanism from the previous design having 3-PRR kinematic structure in [12] is that we have used 4-bar linkages composed of circular flexure hinges for prismatic joints instead of using linear actuators and flexible beams. In short, we have designed the prismatic joint using flexure hinges and embedded in the mechanism shown in Fig. 2b. Circular notch flexure hinges shown in Fig. 2b are used as revolute joints in the mechanism.

The stage is actuated by piezoelectric actuators which drive the prismatic joints by creating forces F_1, F_2 and F_3 and create the center displacements in the direction of u_1, u_2 and u_3 vectors respectively as shown in Fig. 2c. By the combination of the "u" displacements desired x-y motion of the triangular stage can be generated. We will only deal with the x-y motion of the stage because of our capability for measuring the end-effectors position although it has a rotation capability in the z axis as well. We will use this redundancy of the mechanism to increase the range of the stage.

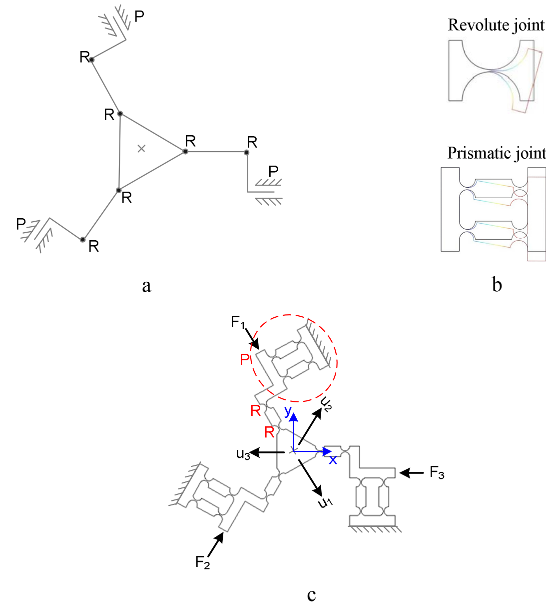

Fig. 2. a. 3-PRR kinematic structure, b. Flexure joints, c.3-PRR compliant stage.

A hexagonal case is also designed outside the mechanisms range so that it can be fixed to the experimental setup properly. The mechanism shown in Fig. 3 is manufactured by using wire electrical discharge machining (Wire EDM) technique by using Aluminum 7075. The shortest thickness of the flexure is 0.8 mm and the overall thickness of the mechanism in z axis is 10 mm.

Fig. 3. Manufactured 3-PRR compliant mechanism.

III. The Experiments

A. *The Experimental Setup*

The experimental setup shown in Fig. 4 is composed of the 3-PRR compliant mechanism, three piezoelectric actuators, a base table, six sliding stages with micrometers, a laser position sensor and a middle base. The used piezo motor is piezomechanik's PST 150/5/40 VS10 type which has max stroke 55 µm for semibipolar -30 V/ +150 V activation and 40 µm stroke for unipolar 0V/+150V activation. Piezomechanik's analog amplifier SVR 150/3 is also used for actuating the piezos. PI's P-853 piezoelectric micrometer drives with sliding stages are put in x and y directions according to the links of the mechanisms so that we can manually preload the mechanism and drive the prismatic joints correctly. For the measurement a DL 16-7PCBA3 4mm x 4mm dual axis position sensing diode on a PCB which has an accuracy of 0.06 µm is placed on the triangular effector's center. Meβtechnologie's laser source is assembled on the top of the position sensing diode. We have designed a Butterworth filter having two degrees in denominator and zero degree in the numerator to get reasonable position datas from the sensor. The sample time of running the laser sensor is 10^{-4} s.

The piezo amplifiers inputs and the laser dual axis position outputs are connected to dSPACE 1103 controller board through DACs and ADCs. Control Desktop with C programming is used for CPU calculations for the controller.

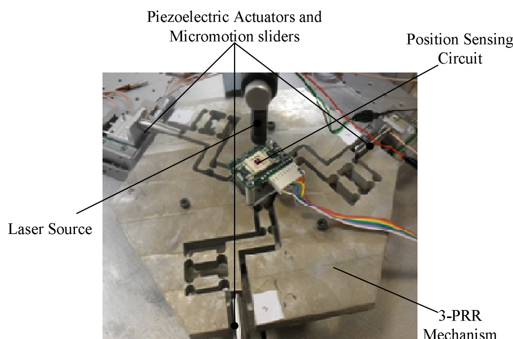

Figure 4. The experimental setup.

B. *Experimentally Determined Kinematics and Workspace*

We have applied respectively 30, 60, 90, 120 and 150 Volts to the piezoelectric actuators when all the piezoelectric actuators are assembled to the mechanism and they are preloaded before starting actuation. The end-effector motion is examined by using the 2D laser position sensor after calibration and filtering the noise from the sensor. The actuators and the direction of the u_1, u_2 and u_3 vectors are shown in Fig 5.

The transformation matrix **A** which relates the motions u_1, u_2 and u_3 to x-y motion of the end-effector can be written as in (1):

$$\begin{bmatrix} x \\ y \end{bmatrix} = \underbrace{\begin{bmatrix} \sin(\theta_1) & \cos(\theta_2) & -\cos(\theta_3) \\ -\cos(\theta_1) & \sin(\theta_2) & \sin(\theta_3) \end{bmatrix}}_{A} \cdot \begin{bmatrix} u_1 \\ u_2 \\ u_3 \end{bmatrix} \qquad (1)$$

The angles of the direction of the u vectors are found as θ_1=25º, θ_2=26º and θ_3=1.5º.

The workspace of 3-PRR compliant mechanism is determined by setting 150 V which provides the maximum strokes (40 µm) to the piezoelectric actuators. The actuations are done individually and by the combinations with each other. The maximum displacement results of the center of the stage is drawn in Fig. 6 which presents a hexagonal workspace. The shape of the hexagonal is distorted so we can say that we have errors due to manufacturing and assembling the mechanism.

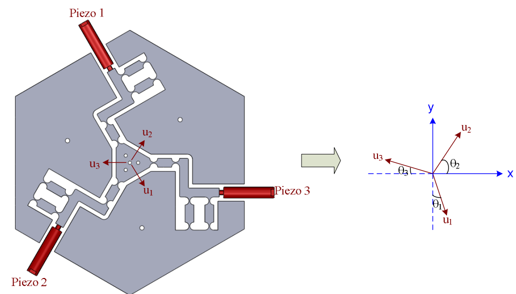

Fig. 5. Motion vectors of 3-PRR compliant mechanism.

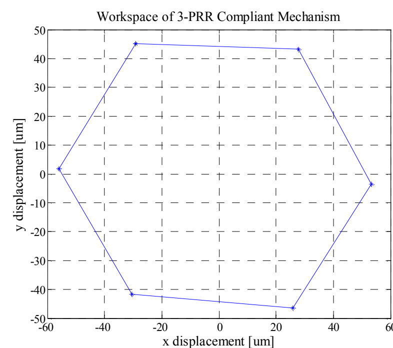

Fig. 6. Experimentally determined workspace of 3-PRR compliant mechanism.

IV. The Contrl Methodology

The control methodology implemented to the mechanism is SMC for the position control which gives us the advantage of being insensitive to the parameter variations that is presented in the system and DOB based on SMC with experimental models to get rid of the uncertainties in the system.

Since the 3-PRR compliant mechanism decouples the stiffness between actuators the system can be treated like 3 Single Input Single Output (SISO) systems resulting u_1, u_2 and u_3 motions as shown in Fig. 5. Firstly, experimental models are extracted which gives the relationship between the applied voltages V(s) and resulting displacements U(s). Then an observer is designed using those experimental models as nominal plants based on SMC. Finally, the position control of the end-effector is succeeded by SMC with the transformation matrix **A**.

A. Experimental Models

Each piezoelectric actuator is actuated by applying a step voltage of 120 V and the end-effector position is measured from dual position sensor in x and y axes. The position measurements are converted into u1, u2 and u3 displacements by using the pseudo inverse matrix A. The "System Identification Toolbox" is used in MATLAB by giving the input results as the applied voltages and the output results which are the displacements in u_1, u_2 and u_3 directions.

The three models are estimated by selecting the transfer function as a second order transfer function in the form of (2). In Fig. 7 the step response of the transfer function between the input voltage to the piezoelectric actuator #1 and the output center displacement measurement is shown as an example. The step responses are slow when compared to a piezoelectric actuator performance which is because of the applied 2nd order filter for the laser sensor measurement to get a reasonable data.

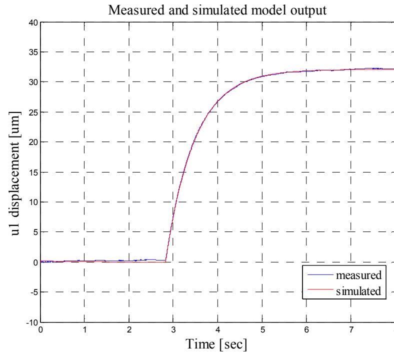

Fig. 7. Step response of u_1 direction and the estimation step response.

$$G_i(s) = \frac{T_{p1}}{(1 + T_{p2} \cdot s)(1 + T_{p3} \cdot s)} \qquad i = 1,2,3 \tag{2}$$

The estimated transfer functions for each actuation direction; $G_1(s)$, $G_2(s)$ and $G_3(s)$ fit the experimental datas in the percentages of %98.92, % 99.44 and % 99.78 respectively. The results for model estimations are presented in Table I.

TABLE I. PARAMETERS OF ESTIMATED TRANSFER FUNCTIONS

Parameters	$G_1(s) = \frac{U_1(s)}{V_1(s)}$	$G_2(s) = \frac{U_2(s)}{V_2(s)}$	$G_3(s) = \frac{U_3(s)}{V_3(s)}$
T_{p1}	80.262	76.305	73.218
T_{p2}	0.65557	0.65228	0.65349
T_{p3}	0.001	0.0034021	0.0038507

B. Observer for Experimental Models

Disturbances of the system can be eliminated by modeling an observer using linear models for each actuation direction. The linear model with nominal parameters can be written as follows:

$$m_{ni}\ddot{u}_i + c_{ni}\dot{u}_i + k_{ni}u_i = T_{ni}v_i - F_{di} \qquad \text{i=1,2,3} \tag{3}$$

According to (3) u_i, m_{ni}, c_{ni}, k_{ni} and v_i are respectively displacement, nominal mass, nominal damping, nominal stiffness and applied voltage of each actuation direction where i represents the number of the direction. T_{ni} is the electromechanical transformation ratio that connects electrical part and mechanical part of the model and F_{di} is the total disturbance. The nominal parameters are extracted from the experimental models presented in Table I for each direction i. F_{di} is the sum of hysteresis force, external force and uncertainties in the plant parameters which are Δm_i, Δc_i, Δk_i and ΔT_i. These parameters are assumed as bounded and continuous. F_{di} can be represented as follows:

$$F_{di} = T_{ni}v_{hi} + F_{exti} + \Delta T_i(v_i + v_{hi}) + \Delta m_i\ddot{u}_i + \Delta c_i\dot{u}_i + \Delta k_i u_i \tag{4}$$

The observer can be designed as a position tracking system, in which F_{di} is replaced with an observer control, $T_{ni}v_{obsci}$, and the observer transfer function is written as:

$$m_{ni}\ddot{\hat{u}}_i + c_{ni}\dot{\hat{u}}_i + k_{ni}\hat{u}_i = T_{ni}v_{ini} - T_{ni}v_{obsci} \tag{5}$$

The parameters for each actuation direction i are presented as follows: $\hat{u}_i$ is the estimated position, v_{ini} is the plant control input, v_{obsci} is the observer control input, where $\hat{u}_i \to u_i$, $F_{di} = T_{ni}v_{obsci}$. Sliding manifolds are selected for each direction i which is $\sigma_i = \dot{u}_i - \dot{\hat{u}}_i + C_{obsi}(u_i - \hat{u}_i)$. The Lyapunov function which provide stability is taken as $v_{Li} = \sigma_i^2/2$ which is positive definite and the derivative of Lyapunov function is taken as $-D_{obsi}\sigma_i^2$, which is negative definite. We will get (6) by equating the above results and simplifying:

$$L_i = \sigma_i\dot{\sigma}_i = -D_{obsi}\sigma_i^2 \Rightarrow \dot{\sigma}_i + D_{obsi}\sigma_i = 0 \tag{6}$$

If we insert sliding mode manifold into the (6):

$$(\ddot{u}_i - \ddot{\hat{u}}_i) + (C_{obsi} + D_{obsi})(\dot{u}_i - \dot{\hat{u}}_i) + C_{obsi}D_{obsi}(u_i - \hat{u}_i) = 0 \tag{7}$$

When we subtract (5) from (4) and insert the result into the above (7) we can find the equivalent controls v_{eqci} which keep system motion in manifold $\sigma_i + D\dot{\sigma}_i = 0$ as follows:

$$v_{ceqi} = \frac{1}{T_{ni}}\begin{Bmatrix} F_{di} + [c_{ni} - m_{ni}(C_{obsi} + D_{obsi})] \\ (\dot{u}_i - \dot{\hat{u}}_i)[k_{ni} - m_{ni}C_{obsi}D_{obsi}](u_i - \hat{u}_i) \end{Bmatrix} \tag{8}$$

According to (8); when $\sigma_i \to 0$ then $u_i \to 0$ and $T_{ni}v_{ceqi} \to F_{di}$. The discrete form of sliding mode control is used as in eqn. 9 for the implementations:

$$v_{i(k)} = v_{i(k-1)} + K_{uobsi}\left(D_{obsi}\sigma_{i(k)} + \frac{\sigma_{i(k)} - \sigma_{i(k-1)}}{dT}\right) \tag{9}$$

K_{uobsi} is a design parameter that optimize the controller and dT is the sampling interval for discrete time control. The system and the observer can be summarized as in (10-12):

$$m_{ni}\ddot{u}_i + c_{ni}\dot{u}_i + k_{ni}u_i = T_{ni}v_{ini} - F_{di} \quad (10)$$

$$m_{ni}\ddot{\hat{u}}_i + c_{ni}\dot{\hat{u}}_i + k_{ni}\hat{u}_i = T_{ni}v_{ini} - T_{ni}v_{obsci} \quad (11)$$

$$v_{ini} = v_{ci} + \frac{\alpha_i}{T_{ni}}v_{obsci} \quad (12)$$

where α_i is a constant for converting the computed voltage value into an input for the dSPACE.

C. SMC for Position Control

A closed loop control is applied for the position control of the center of the triangular stage. The position reference is given in x-y coordinates and the corresponding reference positions, u_{refi} (i=1,2,3), are calculated with the pseudo inverse of the transformation matrix **A** as in (13).

The sliding manifolds for each direction are selected to be as in (14). The discrete forms of SMC applied to the systems are shown in (15) and the systems are described by (16).

$$[u_1 \quad u_2 \quad u_3]^T = \boldsymbol{A}^{\dagger}[x\ y] \quad (13)$$

$$\sigma_{xi} = (\dot{u}_{refi} - \dot{u}_i) + C_{xi}(u_{refi} - u_i) \quad (14)$$

$$v_{i(k)} = v_{i(k-1)} + K_{uxi}\left(D_{xi}\sigma_{x\,i(k)} + \frac{\sigma_{xi(k)} - \sigma_{xi(k-1)}}{dT}\right) \quad (15)$$

$$(\ddot{u}_{refi} - \ddot{u}_i) + (C_{xi} + D_{xi})(\dot{u}_{refi} - \dot{u}_i) + C_{xi}D_{xi}(u_{refi} - u_i) = 0 \quad (16)$$

The full schematic block diagram of the SMC position control with DOB using experimental models is presented in Fig. 8.

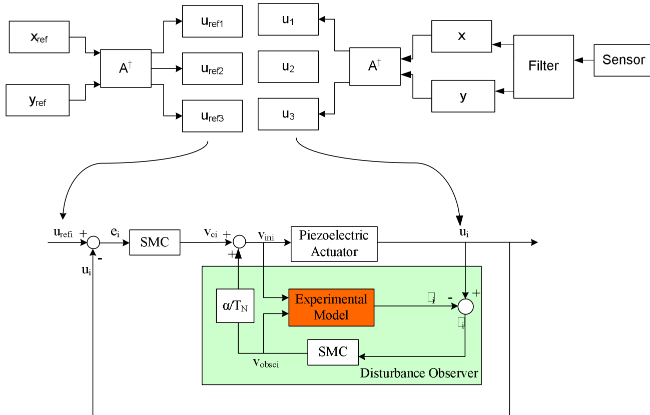

Fig. 8. SMC position control with DOB using experimental models.

V. Results

The position control method is implemented for each actuation direction by coding the calculations in C language according to the control scheme shown in Fig. 8. A circular trajectory has given to the center of the mechanism in order to act as a fine stage that can be used as a laser micro machining stage in the laboratory in which the sample pieces are cut in circular. The diameter of the circle is set as 20 μm and the references in x and y axes are given as:

$$x_{ref} = 10 + 10\sin(0.2\pi t) \quad (17)$$

$$y_{ref} = 10 + 10\cos(0.2\pi t) \quad (18)$$

The pseudo inverse of transformation matrix **A** as in (1) is used for calculating the necessary position references for the u_{ref1}, u_{ref2} and u_{ref3}. The control input voltages is saturated between 0V to 150V to use the bipolar actuation property of the piezoelectric actuators. The SMC parameters for observer and position control are presented in Table II.

TABLE II. SMC for DOB and Position Control Parameters

Sliding Mode Observer Parameters		SMC for Position Parameters	
K_{obs}	2e-6	K_x	2e-2
C_{obs}	1	C_x	40
D_{obs}	50	D_x	3e3

The results of the new method based on experimental models observer are compared with the results based on PEA modes presented in [23]. The implemented control method presented in this paper gives better results according to Figs. 9 and 10 which show the x and y axis errors respectively. The errors in x direction is between -0.15 μm and 0.25 μm as shown in Fig. 9 and the errors in y direction is between 0.06 μm and -0.25 μm as shown in Fig. 10 for the SMC position control with DOB using PEA models. Whereas, when experimental models are used for the DOB the errors in x and y axes are lowered to ± 0.06 μm which is the accuracy of the dual position sensor that is used in laboratory.

It's presented in Fig. 11 how the center of the stage tracks the reference when the proposed control method is implemented.

VI. Conclusion

A compliant stage based on 3-PRR kinematic structure is designed to be used as a micro motion stage for possible micro system applications. The kinematic structure has a compact shape, decouples the stiffness between actuators, and improves the stiffness which leads to the parasitic motions. 4-bar linkages composed of circular flexure hinges are used as prismatic joints and circular flexures are used as revolute joints for the structure. Piezoelectric actuators are used to drive the prismatic joints. The position measurement of the center of the stage is carried out by using a dual laser position sensor.

The mechanism is manufactured however; the center motion experiments show that it has erroneous motion due to manufacturing and assembly. A transformation matrix is found between the actuation directions and x-y axes. SMC position control with DOB is implemented in order to get rid of these unpredictable errors. The system is treated like having 3 SISO systems since the 3-PRR compliant mechanism decouples the stiffness between actuators. Experimental models extracted from the input step voltages for PEAs and the x-y displacement datas as output. These models are used as linear plants for the DOB in order to remove of disturbances with SMC. The results show that the new control method improves the performance of the compliant stage when the errors in x and y axes are compared with the previous results that we have using only

PEA models for DOB. The new method provides the mechanism to work in the accuracy of the measurement which is ±0.06 µm.

For the future work; the mechanism will be modeled in order to see the center position errors due to uncertainties. A sensor can also be added to the mechanism in order to measure and control the rotation of the stage. Also the position measurement can be changed according to the application.

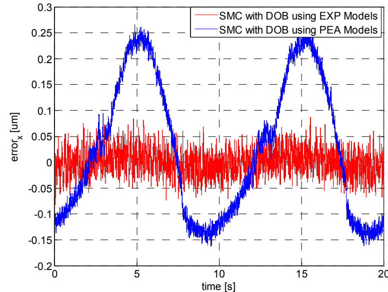

Fig. 9. Errors in x axis.

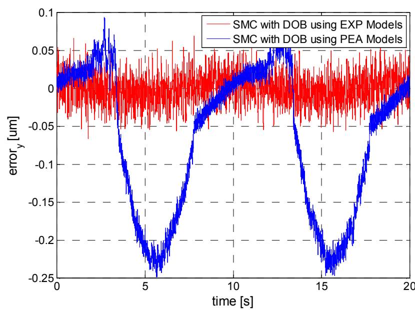

Fig. 10. Errors in y axis.

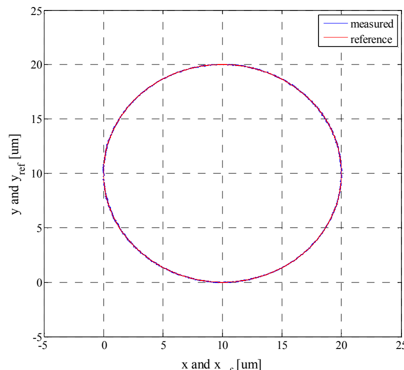

Fig. 11. The reference ad measured x-y motion of the center of 3-PRR compliant mechanism.

REFERENCES

[1] A. H. Slocum, *Precision Machine Design*. New Jersey, USA: Prentice Hall, 1992.

[2] D.G.Chetwynd S.T. Smith, *Foundations of Ultraprecision Mechanism Design*. North Carolina, USA: CRC Press, 1994.

[3] Nicolae Lobontiu, Compliant Mechanisms: Design of Flexure Hinges.: CRC Press, 2003.

[4] Golubovic, E.; Khalil, I.S.M.; Nergiz, A.O.; Baran, E.A.; Sabanovic, A., "Design and control of laser micromachining workstation," Advanced Motion Control (AMC), 2012 12th IEEE International Workshop on , vol., no., pp.1-6, 25-27 March 2012

[5] B. Shirinzadeh, D. Zhang Y. Tian, "Design and dynamics of a 3-DOF flexure-based parallel mechanism for micro/nano manipulation," Microelectronic Engineering, vol. 87, no. 2, pp. 230–241, February 2010.

[6] Daniel C. Handley, Yuen Kuan Yong, Craig Eales Tien-Fu Lu, "A three-DOF compliant micromotion stage with flexure hinges," Industrial Robot: An International Journal, vol. 31, no. 4, pp. 355 - 361, 2004.

[7] W. Szyszkowski, W.J. Zhang B. Zettl, "Accurate low DOF modeling of a planar compliant mechanism with flexure hinges: the equivalent beam methodology," Precision Engineering, vol. 29, no. 2, pp. 237–245, April 2005.

[8] J. Zou, L. G. Watson, W. Zhao, G. H. Zong, S. S. Bi W. J. Zhang1, "The Constant-Jacobian Method for Kinematics of a Three-DOF Planar Micro-Motion Stage," Journal of Robotic Systems, vol. 19, no. 2, pp. 63-72, February 2002.

[9] Tien-Fu Lu, Daniel C. Handley Yuen Kuan Yong, "Loop Closure Theory in Deriving Linear and Simple Kinematic Model for a 3 DOF Parallel Micromanipulator," , Perth, 2003.

[10] Tien-Fu Lu, J. Minase Y. K. Yong, "Trajectory Following with a three-DOF Micro-motion Stage," ,Auckland, 2006.

[11] D.C. Handley, Yuen Kuan Yong Tien-Fu Lu, "Position Control of a 3 DOF Compliant Micro Motion Stage," , 2004.

[12] X. Zhang, J. K. Mills and W. L. Cleghorn, "Dynamic Modeling and Experimental Validation of a 3-PRR Parallel Manipulator with Flexible Intermediate Links", Joutnal of Inteligent & Robotic Systems, vol. 50, no. 4, pp. 323-340, 2007.

[13] Howell L., "Compliant Mechanisms", Wiley New York, 2001.

[14] Howell LL.and Midha A. "A loop closure theory for the analysis and synthesis of compliant mechanisms", Journal of Mechanical Design, Vol. 118, pp: 121-5 (1996).

[15] Tien-Fu Lu; Handley, D.C.; Yuen Kuan Yong , "Position control of a 3 DOF compliant micro-motion stage," Control, Automation, Robotics and Vision Conference, 2004. ICARCV 2004 8th , vol.2, no., pp. 1274-1278 Vol. 2, 6-9 Dec. 2004

[16] Chang J. C., and Her I., "A linear scheme for the displacement analysis of micro-positioning stages with flexure hinges", ASME Journal of Mechanical Design, vol. 116, pp. 770-776, 1994.

[17] Zhang W. J., Zou J., Watson G., Zhao W., Zong G. and Bi S., "Constant-Jacobian method for kinematics of a 3-DOF planar micro-motion stage", Journal of Robotic Systems, Vol. 19, No 2, pp. 63-79, 2002.

[18] Tien-Fu Lu, Daniel C. Handley, Yuen Kuan Yong, Craig Eales, "A three-DOF compliant micromotion stage with flexure hinges", Industrial Robot: An International Journal, Vol. 31 Iss: 4, pp.355 – 36, 2004.

[19] Fite, K.; Goldfarb, M.; , "Position control of a compliant mechanism based micromanipulator ," Robotics and Automation, 1999. Proceedings. 1999 IEEE International Conference on , vol.3, no., pp.2122-2127 vol.3, 1999.

[20] H. C.Liaw, B Shirinzadeh, J. Smith, "Robust motion tracking control of piezo-driven flexure-based four-bar mechanism for micro/nano manipulation",2007.

[21] Shieh, H.J.; Huang, P.K.; , "Adaptive Tracking Control of a Piezoelectric Micropositioner," Industrial Electronics and Applications, 2006 1ST IEEE Conference on , vol., no., pp.1-5, 24-26, May 2006

[22] S.H. Chang, C.K. Tseng and H.C. Chien, An ultra-precision XYθz piezo-micropositioner. Part II. Experiment and performance. IEEE Transactions on Ultrasonics, Ferroelectrics, and Frequency Control, 46 4, pp. 906–912, 1999.

[23] Acer, M.; Sabanovic, A.; , "Sliding-mode control of a flexure based mechanism using piezoelectric actuators," Advanced Motion Control (AMC), 2012 12th IEEE International Workshop on , vol., no., pp.1-6, 25-27 March 2012.